Geochemical Journal, Vol. 52, pp. e7 to e14, 2018 doi:10.2343/geochemj.2.0519

EXPRESS LETTER

Spatial variation of isotopic compositions of snowpack nitrate related to post-depositional processes in eastern Dronning Maud Land, East Antarctica

KAZUSHI NORO,[1] SHOHEI HATTORI,[2]* RYU UEMURA,[3] KOTARO FUKUI,[4] MOTOHIRO HIRABAYASHI,[5] KENJI KAWAMURA,[5] HIDEAKI MOTOYAMA,[5] NORIMICHI TAKENAKA[1] and NAOHIRO YOSHIDA[2,6]

[1]Graduate School of Engineering, Osaka Prefecture University, Osaka 599-8531, Japan
[2]Department of Chemical Science and Engineering, School of Materials and Chemical Technology, Tokyo Institute of Technology, Kanagawa 226-8502, Japan
[3]Department of Chemistry, Biology and Marine Science, Faculty of Science, University of the Ryukyus, Okinawa 903-0213, Japan
[4]Tateyama Caldera Sabo Museum, Toyama 930-1405, Japan
[5]National Institute of Polar Research, Tokyo 190-8518, Japan
[6]Earth-Life Science Institute (ELSI), Tokyo Institute of Technology, Tokyo 152-8550, Japan

(*Received November 16, 2017; Accepted January 23, 2018; Online published March 9, 2018*)

To evaluate post-depositional loss from the snow surface and subsequent redistribution of nitrate, we determined the spatial variation of nitrate concentrations, as well as $\delta^{15}N$ and $\Delta^{17}O$ values of nitrate in surface snow, sampled along a latitudinal transect in eastern Dronning Maud Land, East Antarctica. The NO_3^- concentrations of surface snow ranged from 40.0 to 130.8 μg L^{-1}, showing no obvious trends with latitude, while the $\delta^{15}N(NO_3^-)$ in surface snow increased from coastal sites to inland sites, ranging from –19.4 to 165.5‰. The relationship between the isotopic values ($\delta^{15}N$ and $\Delta^{17}O$) of nitrate and snow accumulation rate are consistent with other traverses studied in East Antarctica (e.g., from Dumont d'Urville station to Vostok, and from East Antarctic coast to Dome Argus), implying that post-depositional loss and redistribution occur similarly throughout East Antarctica.

Keywords: nitrate, photolysis, $\delta^{15}N$, Antarctica, snowpack

INTRODUCTION

Nitrate ($HNO_3(g)$ + p-NO_3^-) is one of the final oxidation products of reactive nitrogen species (NO_y: NO, NO_2 and HONO) in the atmosphere; it is also one of the major ions found in polar ice cores. Therefore, nitrate in ice cores is a potential proxy for NO_y levels in the atmosphere of the past (Dibb *et al*., 1998). Solar variability on centennial to millennial time scales may imprint on the long-term NO_3^- record, as suggested by Traversi *et al*. (2012) in their work on the Talos Dome core record. However, a hypothesis linking NO_3^- spikes to Solar Energetic Particle (SEP) events has recently been discredited (Duderstadt *et al*., 2016; Wolff *et al*., 2012, 2016). A fundamental difficulty in interpreting the concentration of nitrate in ice cores is that nitrate is not stable after deposition to the snow surface, especially at sites with low snow accumulation (Blunier *et al*., 2005; Frey *et al*., 2009), which leads to net loss and redistribution within the snowpack (Frey *et al*., 2009; Jacobi and Hilker, 2007; Röthlisberger *et al*., 2000). The relative importance of post-depositional loss processes, i.e., volatilization of nitric acid (HNO_3) and photolysis of nitrate, has long been debated (Blunier *et al*., 2005; Röthlisberger *et al*., 2000). However, using the stable isotopic composition of nitrate in snow, it has recently been shown in field, laboratory and model experiments that nitrate loss is driven by UV photolysis dominates, especially under cold conditions (Berhanu *et al*., 2014; Erbland *et al*., 2013; Frey *et al*., 2009). HNO_3 volatilization and associated isotopic fractionation may become important at warmer temperatures, greater than –20°C (Erbland *et al*., 2013). To date, attention has focused on the spatial variability of photolytic NO_3^- loss from surface snow in East Antarctica. This variability has been investigated along a traverse between the Dumont d'Urville station (in Adelie Land) and Vostok, passing through Dome C (Erbland *et al*., 2013), as well as along one from the East Antarctic coast to Dome Argus (Shi *et al*., 2015). Based on these studies, it is apparent that, at low accumulation sites, nitrate photolysis results in decreased nitrate concentration in the surface snow, from hundreds to tens of μg L^{-1} below a depth of 10 cm, and

*Corresponding author (e-mail: hattori.s.ab@m.titech.ac.jp)

with $\delta^{15}N(NO_3^-)$ values correspondingly increased. Spatial variation in NO_3^- concentrations and nitrate isotopic compositions ($\delta^{15}N(NO_3^-)$, $\delta^{18}O(NO_3^-)$ and $\Delta^{17}O(NO_3^-)$) in snowpack along a latitudinal transect between Syowa and Dome Fuji station have not previously been investigated. This study investigates such spatial variation in eastern Dronning Maud Land, East Antarctica, for comparison with results from other traverses.

Materials and Methods

Sampling sites

Snow samples were collected in eastern Dronning Maud Land, during the 54th and 57th Japanese Antarctic Research Expedition (JARE). On JARE54, surface snow samples were collected along a coastal-inland traverse, between 25 November 2012 and 13 January 2013 (Fig. 1). Samples were collected and measured throughout the entire depth of between 0 to 30, 50, or 80 cm, as summarized in Table 1. Prior to nitrate measurements, the same melted snow samples were used for sulfur isotopic measurements (Uemura *et al.*, 2016) and subsequently stored for about six months at 4°C, until nitrate was measured. Coastal snow samples were collected during JARE57 at six sites (S30, H42, H68, H80, H108 and H128), between 30 January 2016 and 5 February 2016 (Fig. 1). These were stored at –20°C until the nitrate measurements—from the surface to a depth of 50 cm—were made.

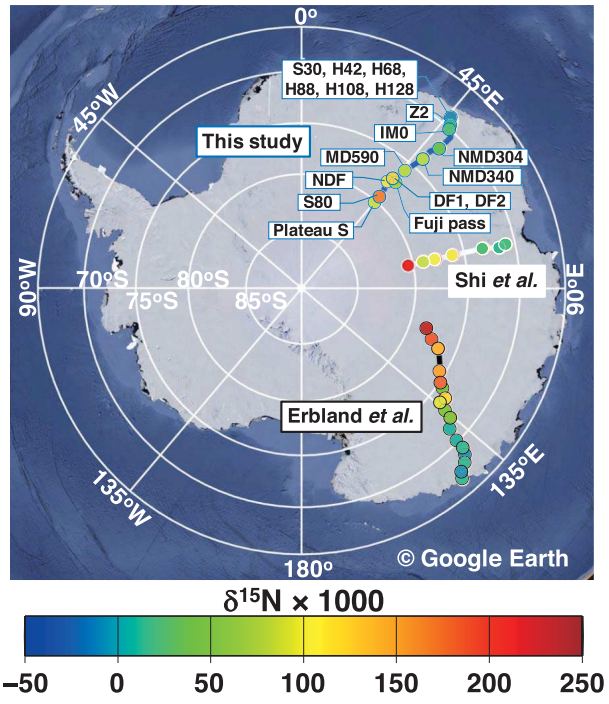

Fig. 1. Spatial distribution of $\delta^{15}N(NO_3^-)$ in surface snow. Snow sampling sites are along traverses from Syowa to Dome Fuji, from French Dumont d'Urville station to Vostok, and from the East Antarctic coast to Dome A. The map was generated using Google Earth (https://www.google.co.jp/intl/ja/earth/).

Chemical and isotopic analyses

The concentrations of SO_4^{2-}, Cl^-, NO_3^-, $CH_3SO_3^-$, Na^+, Ca^{2+}, Mg^{2+}, K^+, and NH_4^+ were measured using an ion chromatograph (Dionex ICS-5000+; Thermo Fisher Scientific, Waltham, MA, USA) at the National Institute of Polar Research. To carry out stable isotope analyses, the NO_3^- in ice samples was separated from other ions using ion chromatography. In our setup, the outflow was collected by a fraction collector (CHF122SC; Advantec MFS, Inc., Dublin, CA, USA), as described in our previous study of coastal Antarctic aerosols (Ishino *et al.*, 2017). The sample was pumped at a flow rate of ~1 mL min^{-1} to a pre-concentration column (IonPac AG15, 4 × 50 mm; Dionex Corp., Sunnyvale, CA, USA). Once the sample was loaded onto the concentration column, anions were eluted using a KOH eluent under a gradient mode. Anions were passed through a guard column (IonPac AG19, 4 × 50 mm; Dionex Corp.) and a separation column (IonPac AS19, 4 × 250 mm, Dionex Corp.). In order to test for possible changes in isotopic compositions of NO_3^- during ion chromatographic (IC) separation, we compared results—with or without IC separation—of reference materials USGS 32, 34 and 35, prepared in 18.2 MΩ cm water (Supplementary Table S1). The differences between with and without IC separation were slightly correlated with isotopic compositions. Sample measurements were therefore also calibrated by using the correlation slope, for measuring $\delta^{15}N(NO_3^-)$, $\delta^{18}O(NO_3^-)$ and $\Delta^{17}O(NO_3^-)$, in order to avoid bias.

Isotopic compositions of NO_3^- in solution were measured using a bacterial method, coupled with N_2O decomposition via microwave-induced plasma (MIP) (Hattori *et al.*, 2016). Briefly, 100 nmol NO_3^- was converted to N_2O by a strain of denitrifying bacteria, having no N_2O reductase. The N_2O produced was then isolated using chemical traps and gas chromatography; it was decomposed to O_2 and N_2 using MIP. The isotopic compositions of O_2 and N_2 were measured using isotope-ratio mass spectrometry (MAT253; Thermo Fisher Scientific). Isotopic reference materials, as well as USGS 32, 34, 35, and their mixtures, prepared in 18.2 MΩ cm water, were also analyzed using the same analytical process as our samples, for normalization. Stable isotopic compositions are reported as: $\delta X = R_{sample}/R_{reference} - 1$, where X denotes ^{15}N, ^{17}O, or ^{18}O, and R denotes the isotope ratios $^{15}N/^{14}N$, $^{17}O/^{16}O$, and $^{18}O/^{16}O$, determined for both sample and standard materials. The δ values are reported as per mil (‰). The $\delta^{15}N$ value is relative to atmospheric N_2 (air), whereas $\delta^{18}O$ and $\delta^{17}O$ values are relative to Vi-

Table 1. Sample location, sampling date, altitude, latitude, longitude, depth, $[NO_3^-]$, $\delta^{15}N$, $\delta^{18}O$, $\Delta^{17}O$, and traverse information for sites mentioned in this study. DF 1 and 2 denote the Dome Fuji station, where a deep ice core was drilled (Dome Fuji Ice Core Project Members, 2017).

Location	Sampling date D.M.Y.	Sampling elevation (m, a.s.l.)	Latitude (°S)	Longitude (°E)	Depth (cm)	$[NO_3^-]$ (μg L^{-1})	$\delta^{15}N$ (‰)	$\delta^{18}O$ (‰)	$\Delta^{17}O$ (‰)	Traverse
Z2	25 Nov 2012	1924	70.0	42.4	0–80	52.3	20.6	69.1	27.4	JARE54
IM0	27 Nov 2012	2215	70.7	44.3	0–50	102.5	25.7	66.1	26.9	JARE54
NMD196	3 Dec 2012	2845	72.2	44.3	0–50	79.8	N.D.	N.D.	N.D.	JARE54
NMD304	5 Dec 2012	3192	73.1	42.9	0–50	69.5	41.1	55.4	24.1	JARE54
NMD370	8 Dec 2012	3338	74.1	43.0	0–50	83.1	N.D.	N.D.	N.D.	JARE54
MD590	12 Dec 2012	3684	76.0	41.1	0–50	104.1	83.5	68.8	31.9	JARE54
DF1	20 Dec 2012	3803	77.3	39.7	0–30	94.0	127.3	51.3	29.4	JARE54
NDF	25 Dec 2012	3763	77.8	39.1	0–30	71.2	111.7	44.0	24.9	JARE54
Plateau S	28 Dec 2012	3678	79.4	40.5	0–30	80.3	165.5	37.5	24.5	JARE54
S80	2 Jan 2013	3625	80.0	40.5	0–30	130.8	90.7	37.7	20.3	JARE54
Fuji pass	8 Jan 2013	3787	77.4	41.5	0–30	92.4	74.3	19.8	13.2	JARE54
DF2	13 Jan 2013	3803	77.3	39.7	0–30	79.8	118.6	25.0	18.7	JARE54
S30	3 Feb 2016	986	69.0	40.7	0–50	40.0	–19.0	75.8	28.2	JARE57
H42	3 Feb 2016	1101	69.1	40.9	0–50	65.4	–6.6	85.5	30.8	JARE57
H68	3 Feb 2016	1164	69.2	41.1	0–50	66.5	–14.5	82.3	28.8	JARE57
H88	3 Feb 2016	1244	69.3	41.2	0–50	124.3	–19.4	83.7	30.3	JARE57
H108	3 Feb 2016	1315	69.3	41.4	0–50	87.9	–6.4	77.8	30.0	JARE57
H128	30 Jan 2016	1376	69.4	41.6	0–50	38.5	14.1	91.0	34.5	JARE57

N.D.: not determined.

enna Standard Mean Ocean Water (VSMOW). $\Delta^{17}O$ notation is used in this study to identify mass-independent fractionation of oxygen, which causes deviation from a mass-dependent fractionation line. $\Delta^{17}O$ is defined here by the linear approximation $\Delta^{17}O = \delta^{17}O - 0.52 \times \delta^{18}O$. By propagating analytical uncertainties for the IC separation and replicate isotopic measurements of USGS 34, 35 and 32, the estimated combined uncertainties were 0.6‰, 1.8‰, and 0.3‰ for $\delta^{15}N(NO_3^-)$, $\delta^{18}O(NO_3^-)$ and $\Delta^{17}O(NO_3^-)$, respectively.

Results

Figure 2 shows altitude, snow accumulation rate (A), NO_3^- concentrations, and $\delta^{15}N(NO_3^-)$ values for each sampling site plotted against latitude. Values for A decrease with increasing elevation, from coastal to inland sites (Figs. 2a and 2b; data are from Hoshina *et al*., 2016). NO_3^- concentrations in surface snow from coastal to inland sites ranged from 38.5 to 130.8 μg L^{-1}, without any specific trend with latitude (Fig. 2c). A wide variation in $[NO_3^-]$ in surface snow at coastal sites was observed during JARE57, having values from 38.5 to 124.3 μg L^{-1} (Table 1). In contrast, a narrow range in $[NO_3^-]$ was observed at inland sites on JARE54, having values from 71.2 to 130.8 μg L^{-1} (Table 1). Along a previous traverse between Syowa to Dome Fuji (Suzuki *et al*., 2003), NO_3^- concentrations at inland sites were 430 ± 100 μg L^{-1}, approximately four times higher than those observed in this study. This difference can be explained by the different sampling depth of Suzuki *et al*. (2003) (surface ~ 3 cm) compared with this study (0–30 cm). As explained below, our $\delta^{15}N(NO_3^-)$ results indicate that NO_3^- concentrations were influenced by post-depositional loss. The $\delta^{15}N(NO_3^-)$ in surface snow clearly increases from –19.4 to 165.5‰ along this transect, moving from low- to high-latitudes (Figs. 1 and 2d). The $\delta^{15}N(NO_3^-)$ values observed in costal surface snow on JARE57 and JARE54 were –19.4 to –6.4‰ and 20.6 to 25.7‰, respectively. Meanwhile, the $\delta^{15}N$ values observed in inland surface snow on JARE54 were 41.0 to 165.5‰.

Discussion

Spatial variation of nitrate and its isotopic composition in East Antarctica

To explain the increasing trend in $\delta^{15}N(NO_3^-)$ values (Fig. 2d) with elevation, it is necessary to consider nitrogen source, post-depositional loss (through photolysis and sublimation) and redistribution of re-emitted NO_y. Atmospheric measurements on the Antarctic coast at Halley show that organic NO_y (CH_3NO_3 and PAN) dominate in

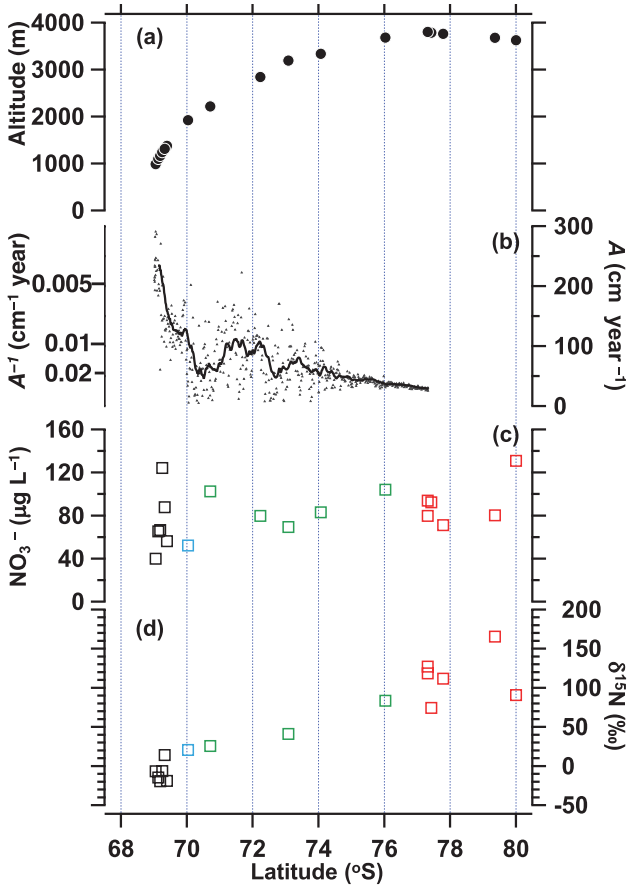

Fig. 2. Altitude (a), snow accumulation rate (Hoshina et al., 2016) (b), nitrate concentration (c), and nitrogen isotopic composition of nitrate (d) as a function of latitude within East Antarctica. For (c) and (d), colors of plots represent the sampling depth and Traverse (Black: JARE57 (0–50 cm), Blue: JARE54 (0–80 cm), Green: JARE54 (0–50 cm) and Red: JARE54 (0–30 cm)).

winter and are consistent with an oceanic source (Jones *et al.*, 2011). However, surface snow nitrate strongly correlates with inorganic NO_y (especially HNO_3) (Jones *et al.*, 2011), indicating that the snow nitrate is dominated by HNO_3. Degradation products of organic nitrate can form nitrate only indirectly, via NO_x production (e.g., see introduction in Savarino *et al.*, 2007). Further inland, on the high Plateau, the influence of tropospheric sources would become less important, especially in winter, and the stratospheric inputs dominate, as supported by isotope measurements (Savarino *et al.*, 2007; Wagenbach *et al.*, 1998). Therefore, the main source of nitrate is from UV destruction of nitrous oxide (N_2O) in the stratosphere. In this study the initial $\delta^{15}N(NO_3^-)$ was calculated as $\delta^{15}N$ (particle NO_3^-) $\approx \delta^{15}N(HNO_3) \approx \delta^{15}N(NO) = 19 \pm 3‰$ (Savarino *et al.*, 2007). Once deposited, this nitrate is influenced by UV photolysis, whereby the $^{14}NO_3^-$ isotopologue is removed faster than the $^{15}NO_3^-$ isotopologue (Berhanu *et al.*, 2014), leading to enrichment of $\delta^{15}N(NO_3^-)$ in the remaining nitrate. On the inland Antarctic plateau, we assume that a single and irreversible process of NO_3^- loss occurs, because the physical release such as volatilization of nitrate leads to only a minor net mass loss (Erbland *et al.*, 2013).

To quantify the effect of nitrate loss related to photolysis, the $^{15}N/^{14}N$ fractionation factor ($^{15}\varepsilon$) is expressed, based on a Rayleigh model, as follows: $\ln(\delta^{15}N_R + 1) = {}^{15}\varepsilon \ln f + \ln(\delta^{15}N_0 + 1)$, where $\delta^{15}N_0$ and $\delta^{15}N_R$ denote δ values for initial and remaining NO_3^-, respectively; and f is the remaining mass fraction of NO_3^- (Blunier *et al.*, 2005). The remaining NO_3^- mass fraction f can be evaluated using measured $\delta^{15}N(NO_3^-)$ values from this study, assuming an initial $\delta^{15}N_0$ value of 19 ± 3‰ (Savarino *et al.*, 2007), and an $^{15}\varepsilon$ for UV photolysis of nitrate, based on laboratory experiments simulated for the Dome C site (–47.9 ± 6.8‰, Berhanu *et al.*, 2014). Thus, the remaining nitrate mass fraction was calculated to be 11 ± 5%, 15 ± 6%, 5 ± 3%, 23 ± 8%, 32 ± 9%, and 13 ± 5% for sites DF1, NDF, Plateau S, S80, Fuji Pass, and DF2, respectively. These values are based on stratospheric input only. If tropospheric sources are also significant, the results will need to be revised accordingly.

In contrast, it is oversimplifying to apply only an $^{15}\varepsilon$ related to photolysis of NO_3^-, when calculating f at coastal sites in Antarctica. This is because sublimation and redistribution of recycled NO_y affect both NO_3^- concentrations and $\delta^{15}N(NO_3^-)$. In fact, the $\delta^{15}N(NO_3^-)$ values at coastal sites (S30, H42, H68, H80, H108 and H128) ranged from –18.7‰ to 14.2‰ (Table 1 and Fig. 2d); these values were lower than $\delta^{15}N(NO_3^-)$ values of nitrate from the stratosphere (19 ± 3‰; (Savarino *et al.*, 2007)). This suggests that other factors influence the $\delta^{15}N(NO_3^-)$ deposited at coastal sites. These lower $\delta^{15}N(NO_3^-)$ values can be explained by nitrogen dynamics and the redistribution of nitrate occurring in Antarctica. For example, the $\delta^{15}N(NO_3^-)$ values of atmospheric nitrate in spring in Antarctica are comparatively low ($\delta^{15}N$: –32.7 ± 8.4‰) (Savarino *et al.*, 2007). Such re-emitted NO_y inland transported to coastal sites via katabatic winds would result in lower $\delta^{15}N(NO_3^-)$ values observed in coastal snow. Furthermore, nitrate concentrations observed in the coastal surface snow samples from S30, H42, H68, H88, H108 and H128 along the JARE57 traverse showed a 3-fold variation (Fig. 2c). The $\delta^{15}N(NO_3^-)$ from surface snow at sites S30 to H108 exhibited relatively small variation, ranging from –18.7 to –6.2‰, while the $\delta^{15}N(NO_3^-)$ value at H128 was higher (14.2‰) than for other samples (Fig. 2d; Table 1). Given that $\delta^{15}N(NO_3^-)$ values in the coastal snow are lower than in nitrate from the stratosphere, the low values of $\delta^{15}N(NO_3^-)$ are likely related to the redistribution of nitrate. Thus, the main process determining

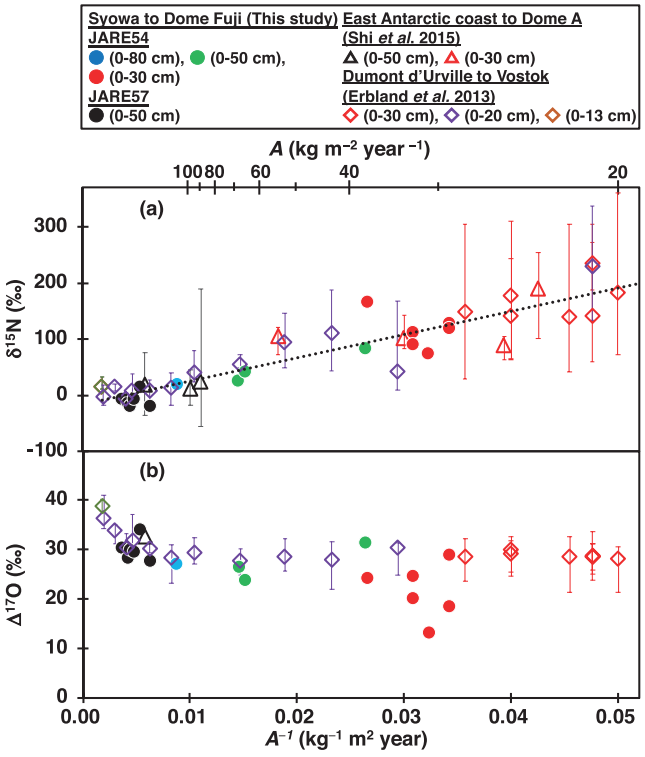

Fig. 3. Values for $\delta^{15}N$ (a) and $\Delta^{17}O$ (b) from nitrate in surface snow as a function of the inverse of the snow accumulation rate A^{-1} (bottom horizontal axis) and the snow accumulation rate A (top horizontal axis). Error bars indicate maximum and minimum values at each pit. A dotted black line in (a) indicates the linear regression line $\delta^{15}N = 4146.2 \times A^{-1} - 15.1$. The $\delta^{15}N$ and $\Delta^{17}O$ for Shi et al. (2015) and Erbland et al. (2013) were recalculated by concentration-weighted averages for matching the core depths of this study. Circles: Syowa to Dome Fuji (JARE54 and 57, This study); Triangles: East Antarctic coast to Dome C (Shi et al., 2015) (0–50 cm and 0–30 cm, respectively); Diamonds: Dumont d'Urville to Vostok (Erbland et al., 2013) (0–30 cm, 0–20 cm and 0–13 cm, respectively).

NO_3^- concentrations in the coastal area is probably the redistribution (i.e., (i) vertical redistribution of NO_3^- within the snowpack driven by nitrate photolysis; (ii) horizontal redistribution via advective transport of emissions (NO_y and HNO_3) and re-deposition further downwind or in near-coastal areas (Savarino *et al.*, 2007; Frey *et al.*, 2009) of re-oxidized NO_y, emitted via photolysis of nitrate in the snowpack, further inland. This explains the inhomogeneity in nitrate concentrations on the surface snow at the coastal sites.

Comparison with other sites in East Antarctica

Figure 3a shows relationships among $\delta^{15}N(NO_3^-)$ and *A* values along three different traverses: from Syowa station to Dome Fuji station (this study), from Dumont d'Urville station to Vostok, passing through Dome C (Erbland *et al.*, 2013), as well as from the East Antarctic coast to Dome A (Shi *et al.*, 2015). The *A* values for Fuji pass, NDF, Plateau S, and S80 were not directly estimated in this study; they were estimated based on an extrapolation of a linear regression between *A* and altitude. The data from Shi *et al.* (2015) were compared as concentration-weighted averages for the same sample depth with our samples. Because sampling depths at the coastal sites of Erbland *et al.* (2013) were not the same as our samples (i.e., they were shallower than 30 cm), a weighted average of all samples measured in their study was calculated (Fig. 3). Given that the contribution of nitrate photolysis is considered to be minor at coastal sites (Savarino *et al.*, 2007), the difference in value related to this sampling depth difference is likely to be small. Overall, the trends in $\delta^{15}N(NO_3^-)$ values and *A* were similar among all three traverses, yielding a regression line with a slope and intercept of 4146.2 ± 279.7 and 15.1 ± 7.4 ($R^2 = 0.84$), respectively (Fig. 3a). We conclude that spatial variation in $\delta^{15}N(NO_3^-)$ is caused by different contributions of UV photolyzed nitrate to the snowpack. This redistribution of nitrate can be characterized as a function of *A* throughout East Antarctica.

The relationship between $\Delta^{17}O$ values of nitrate and *A* along the two JARE traverses (JARE54 and 57; this study), as well as the Erbland *et al.* (2013) traverse and a snow pit from the Shi *et al.* (2015) traverse are shown in Fig. 3b. The $\Delta^{17}O$ values of nitrate collected on JARE57 (S30, H42, H68, H88, H108 and H128) ranged from 27.8 to 34.0‰ (Table 1), which is in good agreement with coastal sites data from Erbland *et al.* (2013) and Shi *et al.* (2015) (Fig. 3b). Results from the samples collected on JARE54 were also generally consistent with those from previous traverses (Fig. 3b). However, values for three samples (S80, Fuji pass, and DF2) ranged from 13.2 to 20.3‰, i.e., lower than for JARE54 and earlier traverses. The sampling dates of DF1 and DF2 differed by several days, whereas the places are only a few meters from each other. In addition, the NO_3^- concentration and $\delta^{15}N(NO_3^-)$ values of samples DF1 and DF2 were similar. Interestingly, there was a large difference of $\Delta^{17}O(NO_3^-)$ between DF1 and DF2. Low $\Delta^{17}O(NO_3^-)$ values of nitrate in the surface snow cannot be explained by the $\Delta^{17}O(NO_3^-)$ values of atmospheric nitrate, which has a summer minimum (~20‰; Savarino *et al.*, 2007). It also is unlikely that analytical errors caused these low $\Delta^{17}O(NO_3^-)$ values, because the measurements of standards and blank were normal. Isotopic exchange between the sample's nitrate and water at some stage during storage or analysis has also been excluded, given that the half-life for oxygen isotope exchange under natural conditions (25°C, pH 7) is estimated to be around 5.5×10^9 years (Kaneko and Poulson, 2013). Thus, it is difficult to ex-

plain these low $\Delta^{17}O(NO_3^-)$ values in S80, Fuji pass, and DF2 samples from JARE54. Similarly unexpected low oxygen isotopic compositions ($\delta^{18}O(NO_3^-)$ values for that study) were also reported in ice cores drilled at Lomonosovfonna, Svalbard (Vega *et al*., 2015). Future study is clearly needed to test the spatial extent and variation of these unexpectedly low oxygen isotope values in snow at inland sites. Perhaps they are related to the spatiotemporal distribution of snow. Except for the low values of $\Delta^{17}O(NO_3^-)$ in nitrate from these three samples, the $\Delta^{17}O(NO_3^-)$ values of nitrate and its relationship to *A* between Syowa and Dome Fuji were generally consistent with other traverses.

Implications for the use of nitrate as an ice core proxy

Nitrate concentrations in the Talos Dome ice core were proposed as a solar activity proxy for the Holocene. Such interpretation is supported by insignificant loss of nitrate in snow pit material at the Talos Dome site (Traversi *et al*., 2012). Based on the linear regression between A^{-1} and $\delta^{15}N(NO_3^-)$ values derived in this study (Fig. 3a), for a snow accumulation rate of *ca*. 72 kg m^{-2} $year^{-1}$ at Talos Dome, the $\delta^{15}N(NO_3^-)$ value at Talos Dome is estimated to be 56.5 ± 8.6‰. This is higher than for nitrate derived from the stratosphere (19 ± 3‰; Savarino *et al*., 2007), suggesting that the Talos Dome site must be influenced by UV photolysis. Whatever the case, reconstruction of past solar activity using nitrate concentrations in ice cores requires careful consideration given that vertical and/or horizontal redistribution of nitrate is occurring in this region.

In addition to $\delta^{15}N(NO_3^-)$ values, it is worth mentioning the possible application of oxygen isotopic compositions of nitrate for the Antarctic samples. Whereas atmospheric nitrate inherits a large positive oxygen isotopic anomaly (^{17}O excess) from ozone, other oxidants such as OH possess lower $\Delta^{17}O$ values. In particular, seasonal variation of $\Delta^{17}O$ values of sulfate and nitrate in coastal Antarctica suggest that $\Delta^{17}O$ values were controlled by oxidant species and not by seasonal changes in $\Delta^{17}O$ values of O_3 (Ishino *et al*., 2017). Thus, the $\Delta^{17}O$ of nitrate in Antarctic ice cores has the potential to reconstruct historical changes in relative abundance of atmospheric O_3 and HO_x over long time periods, based on the WAIS Divide ice core (Sofen *et al*., 2014). However, similar to nitrogen, oxygen isotopic compositions of nitrate are also changed by post depositional processes, especially at sites which have low accumulations of snow. Recently, a chemical model of nitrate behavior at the air-snow interface on the East Antarctic Plateau has been developed, to reconstruct $\Delta^{17}O(NO_3^-)$ values in the atmosphere (Erbland *et al*., 2015). Our new traverse data (Fig. 3b) will provide additional constraints to parameters used in such a chemical model. In turn, this will help establish the mechanisms contributing to the low $\Delta^{17}O(NO_3^-)$ values in inland areas. The determination of past atmospheric $\Delta^{17}O(NO_3^-)$ values from ice core analysis, coupled with global atmospheric chemical transport model such as GEOS-Chem, which quantify atmospheric nitrate formation pathways (Alexander *et al*., 2009), provides the scope for reconstructing past atmospheric oxidizing capacity and its relationship to past global changes.

Summary

We report spatial variations in NO_3^- isotopic compositions from coastal to inland sites in eastern Dronning Maud Land, East Antarctica. Although the NO_3^- concentrations of surface snow between coastal and inland sites ranged from 40.0 to 130.8 μg L^{-1}, without explicit trends with latitude, the $\delta^{15}N(NO_3^-)$ values in the surface snow increased along the traverse from coastal to inland sites, ranging from –19.4 to 165.5‰. Based on a Rayleigh model, the remaining nitrate mass fraction was calculated to vary from 5 to 32% at sites DF1, NDF, Plateau S, S80, Fuji Pass, and DF2. This suggests that, at these inland sites, between 68 and 95% of nitrate was removed via UV photolysis of the snowpack. In contrast, the $\delta^{15}N(NO_3^-)$ values at coastal sites were lower than $\delta^{15}N$ values of stratospheric nitrate, exhibiting a large variation in nitrate concentrations but a small variation in $\delta^{15}N(NO_3^-)$ values. This indicates that the horizontal redistribution via advective transport of nitrate has an important effect on nitrate concentrations in surface snow at coastal sites. The relationship between the isotopic values ($\delta^{15}N(NO_3^-)$ and $\Delta^{17}O(NO_3^-)$) and snow accumulation rate is consistent with previous traverses across East Antarctica, implying that UV-driven post-depositional loss and horizontal redistribution occur similarly throughout East Antarctica.

Acknowledgments—We thank the members of JARE54 and JARE57 traverse teams for assistance with fieldwork. We also thank Kazuki Kamezaki, Asuka Tsuruta, Sakiko Ishino, and Yoshio Nuñez Palma (Tokyo Institute of Technology) for assistance with laboratory experiments and data presentations. Thoughtful and constructive reviews by Becky Alexander and an anonymous reviewer led to significant improvements to the paper. This work is supported by the Japan Society for the Promotion of Science (JSPS): Grants-in-Aid for Scientific Research 16H05884 (S.H.), 16H04947 (S.H.), 26550013 (R.U.), and 17H06105 (N.Y.) from the Ministry of Education, Culture, Sports, Science and Technology (MEXT). The JARE57 traverse was partially supported by the System-inspired Leaders in Material Science (SiMS) Program, and the Program for Leading Graduate Schools of Osaka Prefecture University. We thank Dr. Trudi Semeniuk from Edanz Group (www.edanzediting.com/ac) for editing a draft of this manuscript.

References

Alexander, B., Hastings, M. G., Allman, D. J., Dachs, J., Thornton, J. A. and Kunasek, S. A. (2009) Quantifying atmospheric nitrate formation pathways based on a global model of the oxygen isotopic composition ($\Delta^{17}O$) of atmospheric nitrate. *Atmos. Chem. Phys.* **9**, 5043–5056.

Berhanu, T. A., Meusinger, C., Erbland, J., Jost, R., Bhattacharya, S. K., Johnson, M. S. and Savarino, J. (2014) Laboratory study of nitrate photolysis in Antarctic snow. II. Isotopic effects and wavelength dependence. *J. Chem. Phys.* **140**, 244306.

Blunier, T., Floch, G. L., Jacobi, H.-W. and Quansah, E. (2005) Isotopic view on nitrate loss in Antarctic surface snow. *Geophys. Res. Lett.* **32**, L13501.

Dibb, J. E., Talbot, R. W., Munger, J. W., Jacob, D. J. and Fan, S.-M. (1998) Air-snow exchange of HNO_3 and NO_y at Summit, Greenland. *J. Geophys. Res.: Atmospheres* **103**, 3475–3486.

Dome Fuji Ice Core Project Members (2017) State dependence of climatic instability over the past 720,000 years from Antarctic ice cores and climate modeling. *Sci. Adv.* **3**, e1600446.

Duderstadt, K. A., Dibb, J. E., Schwadron, N. A., Spence, H. E., Solomon, S. C., Yudin, V. A., Jackman, C. H. and Randall, C. E. (2016) Nitrate ion spikes in ice cores not suitable as proxies for solar proton events. *J. Geophys. Res.: Atmospheres* **121**, 2994–3016.

Erbland, J., Vicars, W. C., Savarino, J., Morin, S., Frey, M. M., Frosini, D., Vince, E. and Martins, J. M. F. (2013) Air-snow transfer of nitrate on the East Antarctic Plateau—Part 1: Isotopic evidence for a photolytically driven dynamic equilibrium in summer. *Atmos. Chem. Phys.* **13**, 6403–6419.

Erbland, J., Savarino, J., Morin, S., France, J. L., Frey, M. M. and King, M. D. (2015) Air-snow transfer of nitrate on the East Antarctic plateau—Part 2: An isotopic model for the interpretation of deep ice-core records. *Atmos. Chem. Phys.* **15**, 12079–12113.

Frey, M. M., Savarino, J., Morin, S., Erbland, J. and Martins, J. M. F. (2009) Photolysis imprint in the nitrate stable isotope signal in snow and atmosphere of East Antarctica and implications for reactive nitrogen cycling. *Atmos. Chem. Phys.* **9**, 8681–8696.

Hattori, S., Savarino, J., Kamezaki, K., Ishino, S., Dyckmans, J., Fujinawa, T., Caillon, N., Barbero, A., Mukotaka, A., Toyoda, S., Well, R. and Yoshida, N. (2016) Automated system measuring triple oxygen and nitrogen isotope ratios in nitrate using the bacterial method and N_2O decomposition by microwave discharge. *Rapid Commun. Mass Spectrom.* **30**, 2635–2644.

Hoshina, Y., Fujita, K., Iizuka, Y. and Motoyama, H. (2016) Inconsistent relationships between major ions and water stable isotopes in Antarctic snow under different accumulation environments. *Polar Sci.* **10**, 1–10.

Ishino, S., Hattori, S., Savarino, J., Jourdain, B., Preunkert, S., Legrand, M., Caillon, N., Barbero, A., Kuribayashi, K. and Yoshida, N. (2017) Seasonal variations of triple oxygen isotopic compositions of atmospheric sulfate, nitrate, and ozone at Dumont d'Urville, coastal Antarctica. *Atmos. Chem. Phys.* **17**, 3713–3727.

Jacobi, H.-W. and Hilker, B. (2007) A mechanism for the photochemical transformation of nitrate in snow. *J. Photochem. Photobiol. A: Chemistry* **185**, 371–382.

Jones, A. E., Wolff, E. W., Ames, D., Bauguitte, S. J. B., Clemitshaw, K. C., Fleming, Z., Mills, G. P., Saiz-Lopez, A., Salmon, R. A., Sturges, W. T. and Worton, D. R. (2011) The multi-seasonal NO_y budget in coastal Antarctica and its link with surface snow and ice core nitrate: results from the CHABLIS campaign. *Atmos. Chem. Phys.* **11**, 9271–9285.

Kaneko, M. and Poulson, S. R. (2013) The rate of oxygen isotope exchange between nitrate and water. *Geochim. Cosmochim. Acta* **118**, 148–156.

Röthlisberger, R., Hutterli, M. A., Sommer, S., Wolff, E. W. and Mulvaney, R. (2000) Factors controlling nitrate in ice cores: Evidence from the Dome C deep ice core. *J. Geophys. Res.: Atmospheres* **105**, 20565–20572.

Savarino, J., Kaiser, J., Morin, S., Sigman, D. M. and Thiemens, M. H. (2007) Nitrogen and oxygen isotopic constraints on the origin of atmospheric nitrate in coastal Antarctica. *Atmos. Chem. Phys.* **7**, 1925–1945.

Shi, G., Buffen, A. M., Hastings, M. G., Li, C., Ma, H., Li, Y., Sun, B., An, C. and Jiang, S. (2015) Investigation of post-depositional processing of nitrate in East Antarctic snow: isotopic constraints on photolytic loss, re-oxidation, and source inputs. *Atmos. Chem. Phys.* **15**, 9435–9453.

Sofen, E., Alexander, B., Steig, E., Thiemens, M., Kunasek, S., Amos, H., Schauer, A., Hastings, M., Bautista, J. and Jackson, T. (2014) WAIS Divide ice core suggests sustained changes in the atmospheric formation pathways of sulfate and nitrate since the 19th century in the extratropical Southern Hemisphere. *Atmos. Chem. Phys.* **14**, 5749–5769.

Suzuki, T., Iizuka, Y., Furukawa, T., Matsuoka, K., Kamiyama, K. and Watanabe, O. (2003) Spatial variability of chemical tracers in surface snow along the route from the coast to 1000km inland at east Dronning Maud Land, Antarctica. *Chinese J. Polar Sci.* **14**, 48–56.

Traversi, R., Usoskin, I. G., Solanki, S. K., Becagli, S., Frezzotti, M., Severi, M., Stenni, B. and Udisti, R. (2012) Nitrate in polar ice: A new tracer of solar variability. *Solar Phys.* **280**, 237–254.

Uemura, R., Masaka, K., Fukui, K., Iizuka, Y., Hirabayashi, M. and Motoyama, H. (2016) Sulfur isotopic composition of surface snow along a latitudinal transect in East Antarctica. *Geophys. Res. Lett.* **43**, 5878–5885.

Vega, C. P., Pohjola, V. A., Samyn, D., Pettersson, R., Isaksson, E., Björkman, M. P., Martma, T., Marca, A. and Kaiser, J. (2015) First ice core records of NO_3^- stable isotopes from Lomonosovfonna, Svalbard. *J. Geophys. Res.: Atmospheres* **120**, 313–330.

Wagenbach, D., Legrand, M., Fischer, H., Pichlmayer, F. and Wolff, E. W. (1998) Atmospheric near-surface nitrate at coastal Antarctic sites. *J. Geophys. Res.: Atmospheres* **103**, 11007–11020.

Wolff, E. W., Bigler, M., Curran, M. A. J., Dibb, J. E., Frey, M. M., Legrand, M. and McConnell, J. R. (2012) The Carrington event not observed in most ice core nitrate records. *Geophys. Res. Lett.* **39**, L08503.

Wolff, E. W., Bigler, M., Curran, M. A. J., Dibb, J. E., Frey, M.

M., Legrand, M. and McConnell, J. R. (2016) Comment on "Low time resolution analysis of polar ice cores cannot detect impulsive nitrate events" by D. F. Smart *et al*. *J. Geophys. Res.: Space Physics* **121**, 1920–1924.

Supplementary Materials

URL (http://www.terrapub.co.jp/journals/GJ/archives/data/52/MS519.pdf)
Table S1